Indian Journal of Geo Marine Sciences
Vol. 51 (09), September 2022, pp. 733-744
DOI: 10.56042/ijms.v51i09.2333

Spatial distribution of radar bright band intensity

R S Jaiswal*, S R Fredrick, K T Lakshmi, M Rasheed & R Dobal
Centre for Study on Rainfall and Radio wave Propagation, Sona College of Technology, Salem – 636 005, India
*[E-mail: rajasrisenjaiswal@gmail.com]

Received 27 May 2021; revised 17 September 2022

A radar bright band is a region of enhanced reflectivity in the radar echo. During precipitation, the falling snowflakes start melting when they encounter a warmer layer below freezing. The snowflakes' refractive index and diameter are higher than the snow above. Below the melting layer, where the melting is over, these snowflakes become raindrops that fall faster. So, the number of drops/volume reduces. Since the back-scattered power from the target is directly proportional to the refractive index of the target and the 6^{th} power of its diameter, the reflectivity in the melting region is higher than above and below it. The paper investigates Bright Band Intensity (BBI) derived from 2A23 V6 of the Precipitation Radar (PR) onboard the Tropical Rainfall Measuring (TRMM) in 35N-35S and 180E – 180W from 1999-2002, 2007, and 2008. The study shows that the bright band's occurrence is more over the ocean (mainly the Pacific) than on the continent. Thus, the Pacific Ocean plays a crucial role in weather and climate. It shows substantial seasonal variations. The BBI minima, in particular, show prominent belts across the two hemispheres and show North-South migration with the season in a direction opposite to the Inter Tropical Convergence Zone (ITCZ) and the solar movement. The longitudinally averaged BBI minima occur in the higher latitudes in both hemispheres. The longitudinally averaged BBI maxima in the Northern Hemisphere (NH) occur at low latitudes, and in the Southern Hemisphere (SH), at high latitudes. The BBI (rainfall) maxima are higher in the winter (summer) hemisphere. The BBI maxima and minima, as also the rainfall maxima and minima, occur in opposite hemispheres. Over a location, the daily BBI maximum does not necessarily correspond to the maximum rainfall. But the maxima of longitudinally averaged BBI and rainfall occur in the same hemisphere, so also the minima.

[**Keywords**: Bright band intensity, Northern hemisphere, Southern hemisphere, TRMM]

Introduction

In the troposphere, the bright band is a region that scatters the radar signal the most[1]. This region often lies below the 0 ^{o}C isotherm height, *i.e.* the freezing level. It is the region where the falling snowflakes start melting into the rain, forming water-coated snow particles. The freezing level is the region between the snow above, and the liquid phase below. When the falling snowflakes pass through a temperature above freezing, they start melting. The region below the bright band, where the melting process is over, consists of falling water droplets. The dielectric constant of water being larger than that of ice, the water-coated snowflakes in the bright band region scatter radar signals more than snow particles above. Below the melting layer, where the melting process is over, the drop concentration per unit volume is lower than in the melting layer as the fall velocity of liquid particles is higher. Thus, the reflectivity in the melting layer is higher than that below and above. Hence, the melting region scatters more signals to the radar, giving rise to a bright band signature in the radar echo. Besides, the reflectivity directly varies with the 6^{th} power of the diameter of the scatterer[1,2]. Particles of bigger size dominate the bright band region than that above and below. Thus, the higher reflectivity in the melting layer is attributed to particle size also.

The bright band is an essential concept in meteorology. Rainfall is estimated from the radar reflectivity using a power-law relation. Eventually, high reflectivity in the bright band region gives rise to an overestimation of rainfall[2-5]. Thus, the bright band plays a decisive role in rainfall estimation. So, knowledge of radar bright band is of immense importance in rainfall estimation. To improve quantitative precipitation estimates, White *et al.*[6] and Lin *et al.*[7] suggested use of different reflectivity versus rainfall relationships in rain events with and without a bright band signature.

The bright band helps identify the position of the freezing level[8], which determines the state of precipitation reaching ground[9-11]. If it is close to the Earth's surface, then the precipitation falls as snow, ice pellets, or freezing rain on the ground, while a higher Freezing Level height (HFL) ensures the precipitation reaches the ground as rain. The observed

precipitation type is likely to depend upon several other factors, *viz*. the vertical temperature, moisture profile, etc.

The knowledge of HFL is an essential parameter in rainfall estimation. It is of immense concern in aviation safety as the presence of supercooled water above leads to aviation hazards[12]. A study reported that variability of freezing level and the bright band is closely related to El Nino and La Nina[13]. Thus, knowledge of freezing level and the bright band is essential in climatology, aviation, weather monitoring, and weather modification.

As per the existing literature, the radar bright band occurs below the freezing level. However, Sen Jaiswal *et al*.[14] reported that the bright band's occurrence below the freezing level is a low latitudinal phenomenon. The study shows that as latitude increases, the probability of a bright band occurring above the freezing level increases. At high latitudes, *viz*. in the Subtropical High-Pressure belt (STHP), the bright band mostly occurs above the freezing level. Fabry & Zawazdki[15] reported that the bright band may go above the latter in severe thunderstorms.

Radar bright band appears to be a characteristic of stratiform rainfall and not that of a convective one[16-19]. However, studies show occurrence of bright band in convective rain[15,20]. In a thunderstorm, supercooled liquid drops may go up due to the strong updraft, giving rise to a bright band high above. The rain type flag '130' of the data product 2A23[(ref. 21)] of the Precipitation Radar (PR) onboard the Tropical Rainfall Measuring Mission (TRMM) satellite categorizes the corresponding rainfall event as 'ambiguous' but may be stratiform despite the presence of a bright band.

The study by Sen Jaiswal *et al*.[14] also shows that the Bright Band Height (BBH) varies with the season and the temperature of a location. It further indicates that the BBH exhibits seasonal oscillations between the NH and SH. Besides, it shows land-ocean contrasts. The maximum BBH mostly lies over the continents, while the minima primarily lie over the oceans[14].

Although extensive studies have been carried out on BBH, its microphysical processes are yet to be understood[22]. Also, an understanding of Bright Band Intensity (BBI) is a grey area. Not much research has taken place in analyzing the BBI. The BBI is the returned back-scattered power at the radar from the bright band region. The radar equation gives the received power back-scattered by a target[1].

The intensity and shape of the bright band depend on the shape and concentration of ice crystals and snowflakes above the melting layer, the melting rate of snowflakes, the maximum size of dissolved particles, and rainfall intensity[23]. Williams *et al*.[24] and Sharma *et al*.[25] reported enhanced radar reflectivity and a significant fall velocity gradient in the presence of a bright band. Mahen *et al*.[26] found that the liquid water content under no bright band and bright band conditions is the same.

The Drop-Size Distribution (DSD) is crucial in the numerical modeling of the microphysics of rainfall[27]. The knowledge of DSD is necessary for understanding rainfall intensity and the type of rainfall[28]. It is also essential to understand the reflectivity-versus rainfall relationship. Besides, the temporal and spatial information of DSD affects rain-induced attenuation[29]. Maitra[30] reported that the prevailing DSD in the tropical region can cause high variability in the rain attenuation distribution, indicating the need for a long-term and extensive measurement of DSD in the tropical region. However, the DSD data are inadequate. As the BBI depends on drop size, its knowledge will give an indirect estimation of drop size[31], which, in turn, will throw light on the type and intensity of rainfall. A study by Huggel *et al.*[31] introduced a parameter called the strength of the bright band and reported that a well-defined (weak) bright band shows a high (low) value of bright band strength. They also related large (weak) values of bright band strength to big (small) drop sizes. They found a negative correlation of 0.6 – 0.7 between the parameters of Marshall-Palmer DSD and bright band strength. However, they noted that the relation between DSD and bright band strength gradually becomes less significant for weaker precipitations[31]. Mahen *et al*.[26] noticed a significant number of small drops and a lower number of large drops under no bright band compared to that in the presence of a bright band. Waldvogel[32] reported a prominent bright band and large drops associated with widespread rain. Studies showed different characteristics of drop size[7,33] and bright band strength[7] in the bright band and non-bright band precipitation. The characteristics of the spatial distribution of precipitation obtained from the knowledge of radar reflectivity improve the Numerical Weather Precipitation (NWP) forecasts,

particularly, in convective precipitation[34].

In this paper, the authors investigate the BBI derived from the data product 2A23 V6 of the PR onboard the TRMM in the latitudinal belt of 36N – 36S and the longitudinal belt of 180W – 180E, during the period 1999, 2000-2002, and 2007-2008.

The authors aim to find i) the daily and monthly variations of the BBI, and whether it oscillates between the NH and SH, with the season; ii) the location where the BBI attains its maximum or minimum value, termed as BBI_{mx} and BBI_{mn}, respectively, and whether there are certain regions in the 36N – 36S latitudinal belt, where the BBI_{mx} or BBI_{mn} frequently occur. In particular, authors attempted to know whether the BBI_{mx} or BBI_{mn} is higher over the ocean compared to the continental mass; iii) the continental locations, where the BBI_{mx} or BBI_{mn} mostly occurs and iv) if the occurrence of the BBI_{mx} or BBI_{mn} has any implications on rainfall.

There were certain issues regarding the reliability of 2A23 V6. The antenna scan angle affects the detected bright band count of the TRMM[35]. The bright band count's reliability was improved a little after the orbit boost of the TRMM in August 2001(ref. 35). Nevertheless, the TRMM proves to be a very useful mission by providing several parameters that are essential in understanding the rainfall mechanism. It is noteworthy that the Global Precipitation Mission (GPM) is an improved mission that observes rain and snow[36]. The GPM serves as a platform to unify precipitation measurements from a constellation of research and operational satellites.

Materials and Methods

The BBI is the power received by the PR from the bright band region. These values are obtained from the data product 2A23(ref. 21) of PR onboard the TRMM, in Hierarchical Data Format (HDF) and converted to ASCII before analysis. It is noteworthy that the TRMM had an overpass at a location once a day, or very rarely, twice. Hence, it overlooked many rainy events. The study covers the latitudinal belt 36N – 36S and longitudinal belt 180E – 180W. The BBI values have been obtained from 1999 to 2002; 2007 and 2008. The BBI values from 2003 to 2006 have not been included in the study as the data were not obtained for this period. The supercomputing facility is used in the present study for the download and conversion of the TRMM data. The study includes investigation of maximum (BBI_{mx}), and minimum (BBI_{mn}) BBI values over a location, on all days for the entire period. In this paper, BBI_{mx} (BBI_{mn}) refers to the maximum (minimum) value of the bright band over a location.

To investigate the relation between rainfall and BBI, the daily rainfall data were obtained from the data product 2A12 of the Tropical Microwave Imager (TMI) onboard the TRMM from 2007 to 2008.

Occurrence of daily BBI

To find the locations of the $BBI_{mx/mn}$, to find whether these occur over the continent or ocean, and to seek the tendency of the same to occur over a certain place, the daily BBI values at each latitude in the region of study were obtained. From the daily values, the maximum/minimum values of the BBI and the corresponding locations were noted. The maximum/minimum values of the BBI are termed as $BBI_{mx/mn}$. Then, over a location, the frequency of occurrence of $BBI_{mx/mn}$ in a month is found. The frequency of occurrence indicates how often it occurs over the location. For example, a higher occurrence of BBI_{mx} over a location indicates that the BBI attained the maximum value over the location more often in comparison to other locations.

Monthly average of longitudinally averaged BBI

To find the locations of the monthly average BBI_{mx} and BBI_{mn} values, averaged over longitudes, the daily longitudinally averaged BBI at a particular latitude were estimated, in intervals of 2 degrees, in the longitudinal range of 180 E – 180 W. From these daily BBI values, the monthly averages of the longitudinally averaged BBI values at particular latitudes were found. From these data, the maximum and minimum BBI values over the region of interest were found. Following this, the location where the $BBI_{mx/mn}$ shows the maximum occurrence is found. Thus, the occurrence of $BBI_{mx/mn}$ in the NH and the SH, and the effect of season on the occurrence of $BBI_{mx/mn}$ were found.

The monthly averages of longitudinally averaged BBI values at an interval of 2 degrees were also used to study the latitudinal variations of BBI in a month.

Results and Discussion

Occurrence of global BBI_{mx} and BBI_{mn}

In an attempt to find where the BBI_{mx} and the BBI_{mn} mostly occur, the daily bright band values over the continents and the oceans in the region of study were investigated, during the entire period of study.

Tables S1 – S2 show the latitude, longitude, and geography of the continental locations where the BBI_{mn} and BBI_{mx} occurred, respectively.

Figure S1 shows the frequency of occurrence of BBI_{mx} in 2000. It reveals that during December – April, the BBI_{mx} mostly occurs in the NH- over the North Pacific, followed by the North Atlantic. From May-November (except September), it mostly occurs in the SH- mainly over the South Pacific, and sometimes over the South Atlantic. In May, the maximum occurrence of BBI_{mx} is seen over the Indian Ocean, followed by the South Atlantic, and the South Pacific. In September, the BBI_{mx} occurs in the NH and SH in 52 % and 48 % of cases, respectively. Observations in other years show that sometimes, it starts becoming higher in the NH from September/October and extends till May (Figs. S2 – S6).

The BBI_{mn} mostly occurs in the NH from December – March and in the SH from April – November in 2000 (Fig. S7). However, investigation in other years (Figs. S8 – S12) shows that in some years, the occurrence of BBI_{mn} starts becoming higher in the NH in November and at times extends up to April/May.

Besides, Figures S1 & S7, respectively show the occurrence of BBI_{mx} and BBI_{mn} over continental locations in 2000. Figures S1 – S12 reveal that although every year, these quantities occur over the continental locations, the occurrence is less than that over the oceans. For example, Figure S1 shows that in January 2000, the BBI_{mx} occurred over Australia, and South Africa in 16 % and 7 % of cases, respectively, while over Mozambique, Argentina, D R Congo, and Iran in 3 % of cases. The BBI_{mn} occurred over the USA, Saudi Arabia, and South Africa in 3 % of cases.

Thus, it appears from Figures S1 – S6 and Figures S7 – S12 that the frequency of occurrence of daily BBI_{mx} and BBI_{mn} over a location depends on seasons. The daily BBI_{mx} mostly occurs in the NH from December – March when the winter season prevails there. During this time, the BBH is higher in SH[14], where the rainy belt lies. During June – September, *i.e.*, northern hemispheric summer, the BBH is higher in the NH, with the prominent rainy belt lying there. During this time, the daily BBI_{mx} mostly occurs in the SH. Thus, it appears that the BBH and rainfall are higher in the summer hemisphere, while the BBI is higher in the winter hemisphere. Also, the occurrence of BBI is higher over oceans in comparison to over the continents. The frequency of occurrence is the highest over the Pacific Ocean. The second-highest appearance of BBI_{mx} /BBI_{mn} is found over the Atlantic Ocean every year.

It is noteworthy that the year 2008 showed a peculiar behavior in the occurrence of BBI_{mx} / BBI_{mn}. Unlike other years, in June 2008, the BBI_{mx} occurred over the continents and oceans in 50 % of cases each (Fig. S6). The BBI_{mn} happened over the oceans and the continents in 59 % and 41 % of cases, respectively (Fig. S12). In July and August, both the BBI_{mx} and the BBI_{mn} always occurred over the oceans. Interestingly, in July and August 2008, the role of the North and the South Pacific in governing the BBI_{mx} interchanged- in July the BBI_{mx} occurred over the North Pacific in 65 % of cases and over the South Pacific in 35 % of cases; while in August, it was just the opposite. The reason behind the unusual behavior of BBI_{mx} / BBI_{mn} in 2008 is not understood yet. It is noteworthy that the year 2007 – 2008 was strong, while 2008 – 2009 was a weak La Nina year[37].

A closer look at Figures S1 – S6 show that during the period of study, the occurrence of BBI_{mx} was higher over the oceans in all months except in June and September 2008; September and October 1999; October 2000, and July 2001 when the occurrence over land was little higher than that over the ocean. The occurrence of BBI_{mx} over land was less but comparable to that over the ocean in June 2000; October 2001; July and November 2007; November 2008; and October 2002 and 2008. It is noteworthy that the year 1998 – 1999, 2000 – 2001, 2007 – 2008, and 2008 – 2009 were La Nina years[37]. Thus, it appears that during the La Nina years, in June – July and September – November, the occurrence of BBI_{mx} increased over land in comparison to normal years. The reason for the increased occurrence of BBI_{mx} over the land during the La Nina years is yet to ascertain.

Occurrence of bright band intensity over land

To find whether the BBI_{mx} or the BBI_{mn} occurs over any particular region in the continental mass, the daily BBI_{mx} and BBI_{mn} values were investigated. The study reveals that the occurrence of BBI_{mx} (Figs. S1 – S6) and BBI_{mn} (Figs. S7 – S12) over the continent shows seasonal variations.

The investigation over the whole period of study further reveals that over the continent, the BBI_{mn} mostly occurs in the USA (31.48 % cases), followed by China and South Africa (22.22 % cases each).

Over South America and Australia, the BBI_{mn} occurs in 14.7 % and 9.2 % of cases, respectively. It also occurs in other parts of Asia, *viz*. Iran, Syria, and Colombo. However, in these places, the occurrence is very less.

The BBI_{mx} mostly occurs in South America (26.86 % of cases), followed by the USA and Africa in 23.88 % of cases. In Australia, India, and China, it occurs in 16.41 %, 5.97 %, and 2.98 % of cases, respectively. Over India, the BBI_{mx} occurs in May, July, August, and October. It occurs in other parts of Asia, *viz*. Yemen, Thailand, and the Philippines. However, in these places, the occurrence is very less.

Shift of $BBI_{mx/mn}$ belt in the northern and southern hemisphere

The study attempted to find the shift of the $BBI_{mx/mn}$ belt from the NH to the SH and vice versa; in particular, to see if it shows seasonal oscillations.

Shift of BBI_{mn}

Figure 1 (a – l) describe the results of the investigation of BBI_{mn}. Figure show that the daily BBI_{mn} almost forms a band on both sides of the equator and shows substantial seasonal variations. From May – October, a prominent band of BBI_{mn} exists in the SH, where winter prevails. During November – March, there is a gradual northward shift of the BBI_{mn} band, implying an increasing occurrence of BBI_{mn} in the NH. Its prominence is seen in the NH till March. In April and November, in both hemispheres, almost parallel bands of BBI_{mn} appear, with a 50 % occurrence in each hemisphere. It is noteworthy that from September – March, the Sun moves from North to South. During April – October, the BBI_{mn} band shifts southward, opposite to that of the solar movement during this period. A study shows that during October-mid May, the ITCZ shifts to the SH, and from June – September, it is in the NH[38]. Thus, the movement of BBI_{mn} is opposite to the seasonal oscillations of the ITCZ. Figure 1 (a – l) show the same results in all years.

Shift of BBI_{mx}

Figure S13 describes the results of the investigation of BBI_{mx}. A prominent band of BBI_{mx} exists in the NH from November – March and in the SH from May – September. In April and October, it occurs in both hemispheres in 50 % of cases each. From April – September, it shifts from the NH to the SH. From October – March, it shifts northward, opposite to that of the solar movement. However, the annual march of BBI_{mx} from North to South, and vice versa is not so prominent as that of the BBI_{mn}. Similar results are seen in all years (Fig. S13). From October – March, the ITCZ, *i.e*., the rainy belt shifts from the NH to the SH, and from June – September, it shifts northward. The shift of the ITCZ is in synchronization with solar movement. Thus, the seasonal oscillation of the BBI from North to South and vice versa is opposite to the ITCZ and solar motion. Besides, the investigation shows that the $BBI_{mx/mn}$ lies predominantly in the winter hemisphere.

Study of monthly average BBI in the northern and southern hemisphere

The investigation helps to know the occurrence of the longitudinally averaged $BBI_{mx/mn}$ in the NH and the SH and their seasonal variations. Figure 2(a & b), respectively describe the occurrence of BBI_{mx} and BBI_{mn}. The tips of the bar in Figure 2(a & b) show the latitude where the monthly average of longitudinally averaged $BBI_{mx/mn}$ occurred. Figure 2(a) shows that during February – May, and December, the monthly average BBI_{mx} mostly occurred in the SH. In June, July, and October, it primarily occurred in the NH. During January, August, September, and November, it sometimes happened in the NH, and sometimes, in the SH.

Figure 2(b) shows that during January – April, the monthly average BBI_{mn} mostly occurred in the NH, while from July – November, the occurrence was higher in the SH. During May, June, and December, it sometimes happened in the NH, and sometimes in the SH.

Figure 2(a & b) further show that the highest BBI_{mx} occurred mostly in the NH, while the lowest BBI_{mn} mainly occurred in the SH.

Longitudinally averaged monthly BBI versus latitude

The monthly average of longitudinally averaged BBI at each latitude was investigated in intervals of 2 degrees, to understand how it varies with latitudes. Figure 3(a – d) show that the BBI_{mx} occurred at 2° N, 8° N, 32° S, and 32° N, respectively, whereas BBI_{mn} occurred at 26° N, 14° N, 20° S, and 18° S, respectively in February 1999, July 2007, September 2001, and October 2002.

Bright band intensity maxima (BBI_{mx})

The investigation reveals that the occurrence of daily longitudinally averaged BBI_{mx} shows seasonal

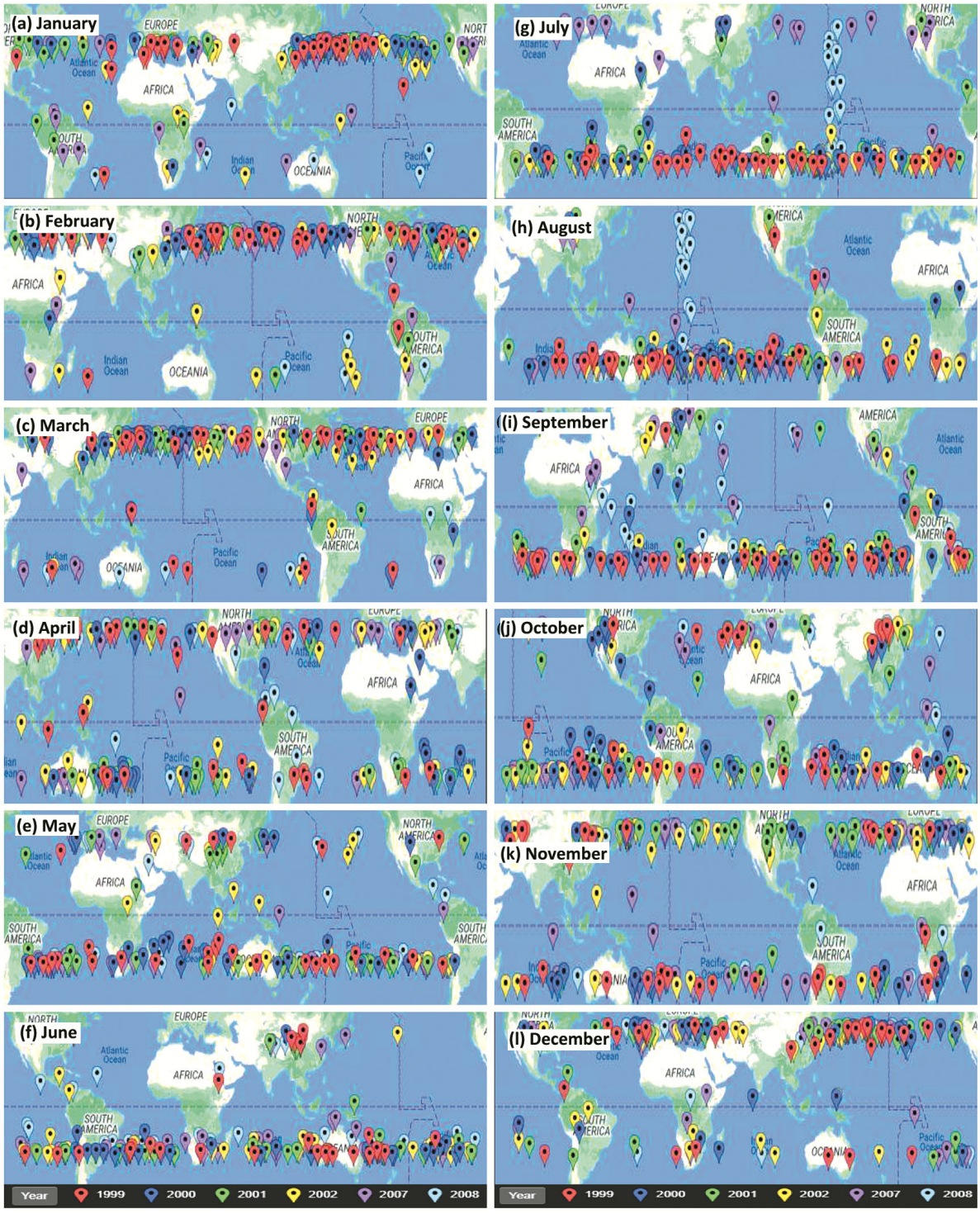

Fig. 1 — (a – l) North-South migration of BBI_{mn} with the season

variations. It mostly occurs in the SH, from February to May, and in the NH from June to November. In December, it occurs in both hemispheres in 50 % of cases each. In January, it occurs at the equator, and in both hemispheres in 33.3 % of cases each (results not shown).

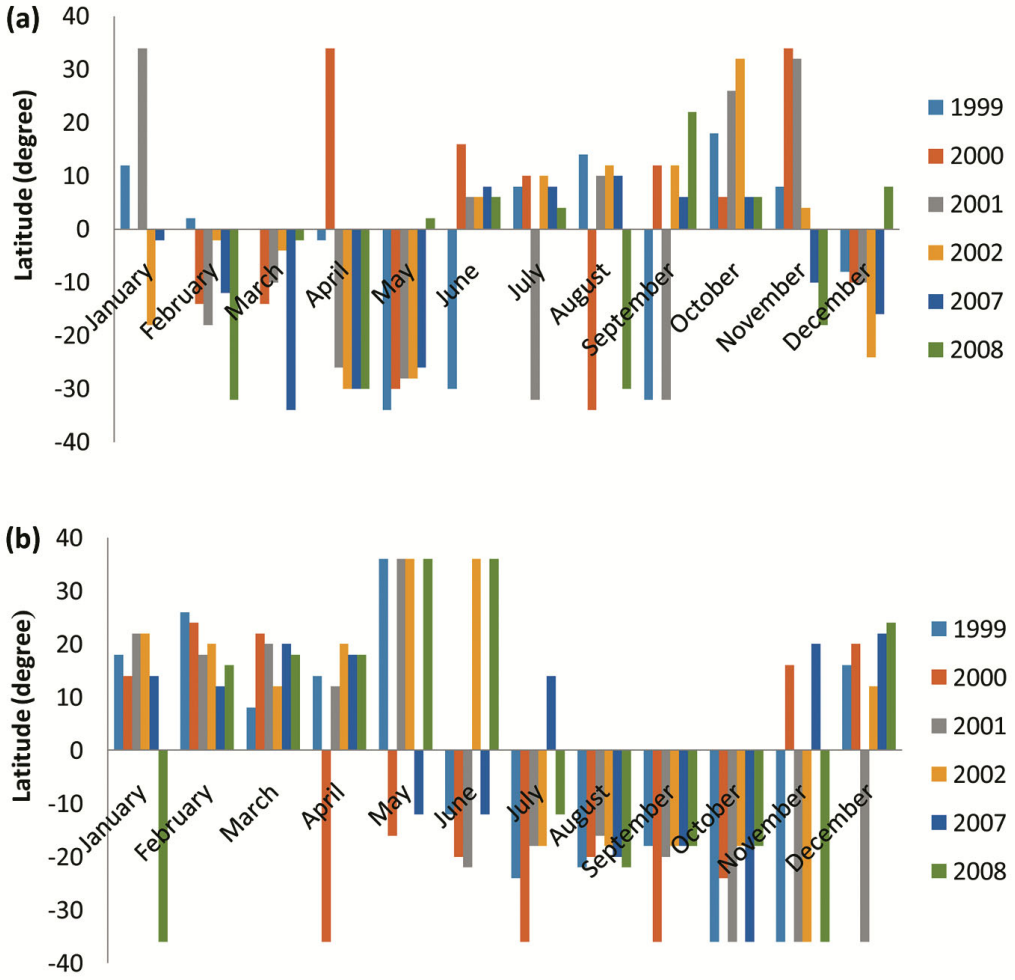

Fig. 2 — Occurrence of the monthly average (a) BBI_{mx}, and (b) BBI_{mn}

Besides, the study shows that in NH, it occurs at ≥ 18° N, in 23.3 % of cases, and at the STHP in 14.71 % of cases, implying that the BBI_{mx} mostly occurs at the lower latitudes in NH. In the SH, it occurs at ≥ 18° S in 60.6 % of cases, and the STHP in 42.4 % of cases, implying that it mostly occurs at high latitudes in SH.

Bright band intensity minima (BBI_{mn})

The longitudinally averaged BBI_{mn} starts showing its occurrence in the NH from November, even though the maximum occurrence is seen in the SH in this month. In December, its occurrence in the NH overtakes. In January – April, it always occurs in the NH. From May, it starts migrating to the SH, while retaining its predominant occurrence in the NH. In June, it mostly occurs in the SH, and from July – October it always remains there (results not shown).

In the NH, it occurs at ≥ 18° N in 66.6 % of cases and at STHP in 16.6 % of cases. In the SH, it occurs at ≥ 18° S in 82.41 % of cases, and in the STHP in 32.3 % of cases, implying that in both hemispheres it occurs at high latitudes, indicating the formation of smaller drop-sizes in comparison to that at low latitudes. The investigation further shows that when the BBI_{mn} occurs in the NH, the BBI_{mx} occurs in the SH and vice versa.

Bright band intensity and rainfall

To understand if the BBI_{mx} or BBI_{mn} corresponds to maximum rainfall, the authors analyzed the variations of longitudinally averaged BBI and longitudinally averaged total monthly rainfall with latitudes in intervals of 10 degrees. The investigation shows that in 2007 the crests (troughs) of one coincide with the crests (troughs) of the other from 30° N – 30° S

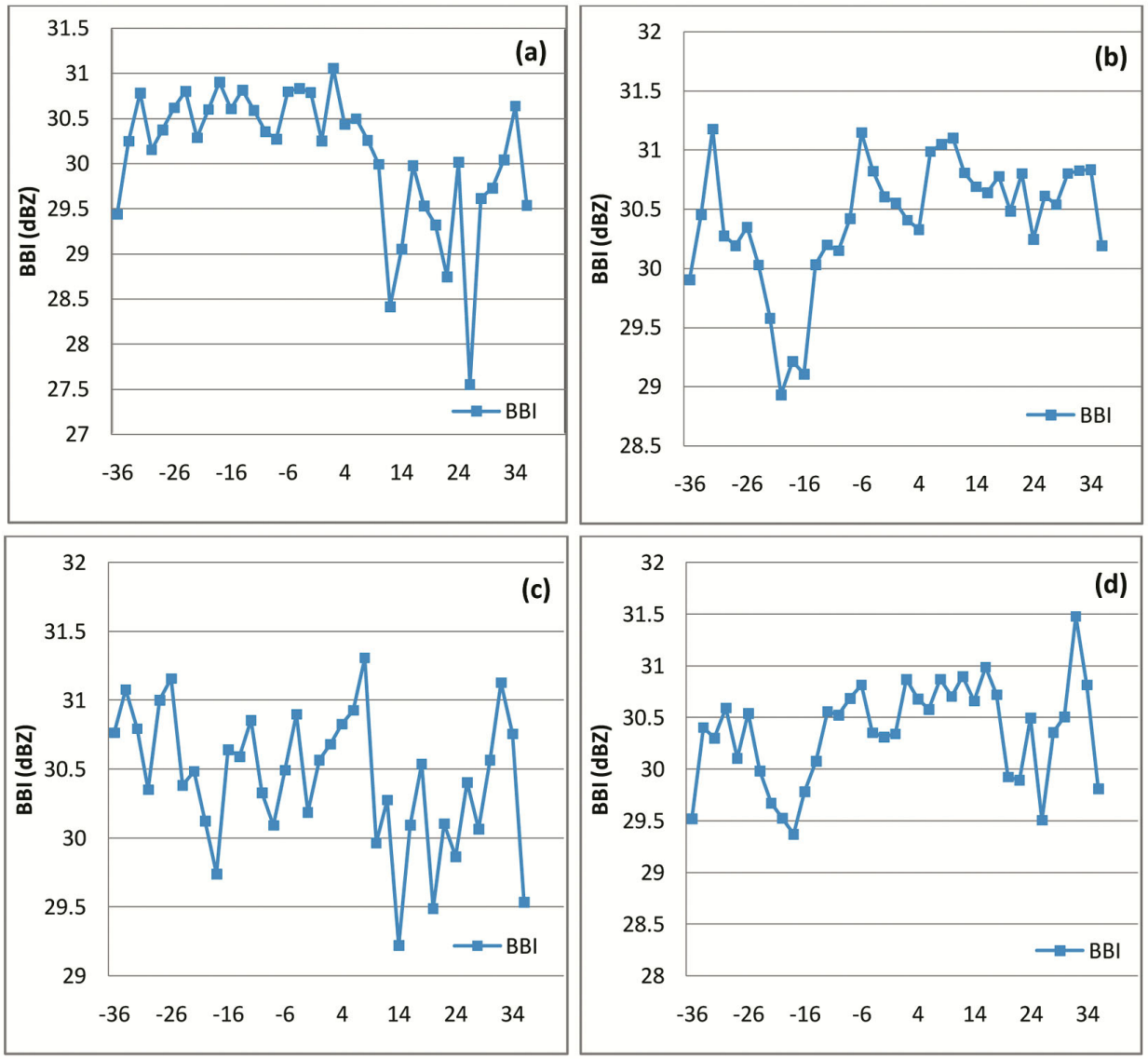

Fig. 3 — Variation of longitudinally averaged monthly BBI with latitude in (a) February 1999, (b) July 2007, (c) September 2001, and (d) October 2002

in March – June, and in July – August, from equator – 30° S. The crests of one superpose with the troughs of the other in the NH in July – August; in the whole of 30° N – 30° S in September – October, and at the equator in December. However, in November – December both match beyond 10° (Figs. S14 – S15). Figure 4(a) shows the variations of BBI and rainfall in May 2007. Results for other months are not shown.

In 2008, these two matches in May, September, and October throughout 30° N – 30° S; and from June – August, and December, these two matches from the equator – 30° S, and in January, March, April, and November from equator – 30° N (Figs. S14 – S15). However, in February, these do not match (Fig. 4b).

To find if the rainfall maxima and the $BBI_{mx/mn}$ occurred in the same hemisphere, the longitudinally averaged monthly BBI and monthly rainfall maxima in the years 2007 and 2008 were investigated. The investigation shows that the rainfall maxima (minima) and the BBI_{mx} (BBI_{mn}) mostly occur in the same hemisphere (Table S3). Table S3 also shows that the rainfall maxima occur in the SH in January – March, and at the equator in April, July, and October – December. In May, June, August, and September

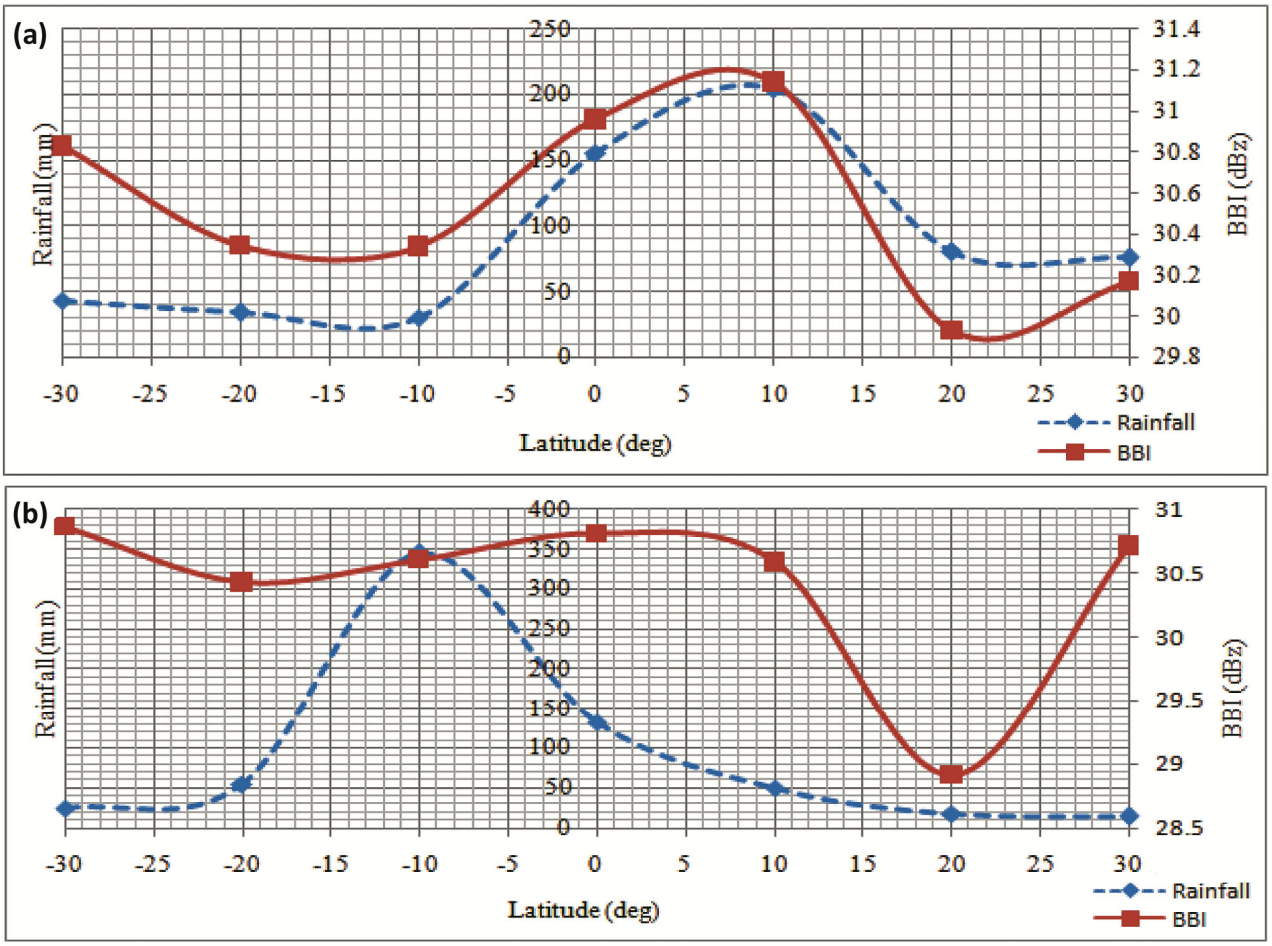

Fig. 4 — Variation of BBI and rainfall with latitude in (a) May 2007, and (b) February 2008

these occur in the NH. During December – April, the rainfall minima occur in the NH, while during May – November, these occur in the SH. Thus, the maximum rainfall occurs in the summer hemisphere, while the rainfall minima occur in the winter hemisphere. Besides, Table S3 shows that when the rainfall maxima occur in the NH, the minima occur in the SH and vice versa. The same observation holds good in the case of BBI_{mx} and BBI_{mn}.

To find if the daily BBI_{mx}/BBI_{mn} and the rainfall maxima occur simultaneously at the same latitude, the variation of BBI and rainfall with latitude on individual days were studied at a fixed longitude. Figure 5(a & b) show the latitudinal variation of both parameters at 70° E on 1 March 2007 and 15 January 2008, respectively. Figure 5(a & b) further represents that the daily BBI and rainfall maxima mostly do not occur at the same latitude. However, on some days, these two superpose. The same result is found in other months and years (results not shown). Thus, it appears that a location showing the highest rainfall at an instant does not correspond to the highest BBI always. But, Table S3 shows that the longitudinally averaged BBI_{mx} and monthly rainfall maxima mostly occur in the same hemisphere.

A high BBI indicates a strong return power from the target. This, in turn, indicates a bigger drop-size[31]. It may further indicate the maximum probability of occurrence of a particular rain type. However, this does not necessarily indicate that the concerned location faces the maximum rainfall. Similarly, the occurrence of BBI_{mn} over a location indicates the presence of smaller drop sizes, but not necessarily a low-intensity rainfall.

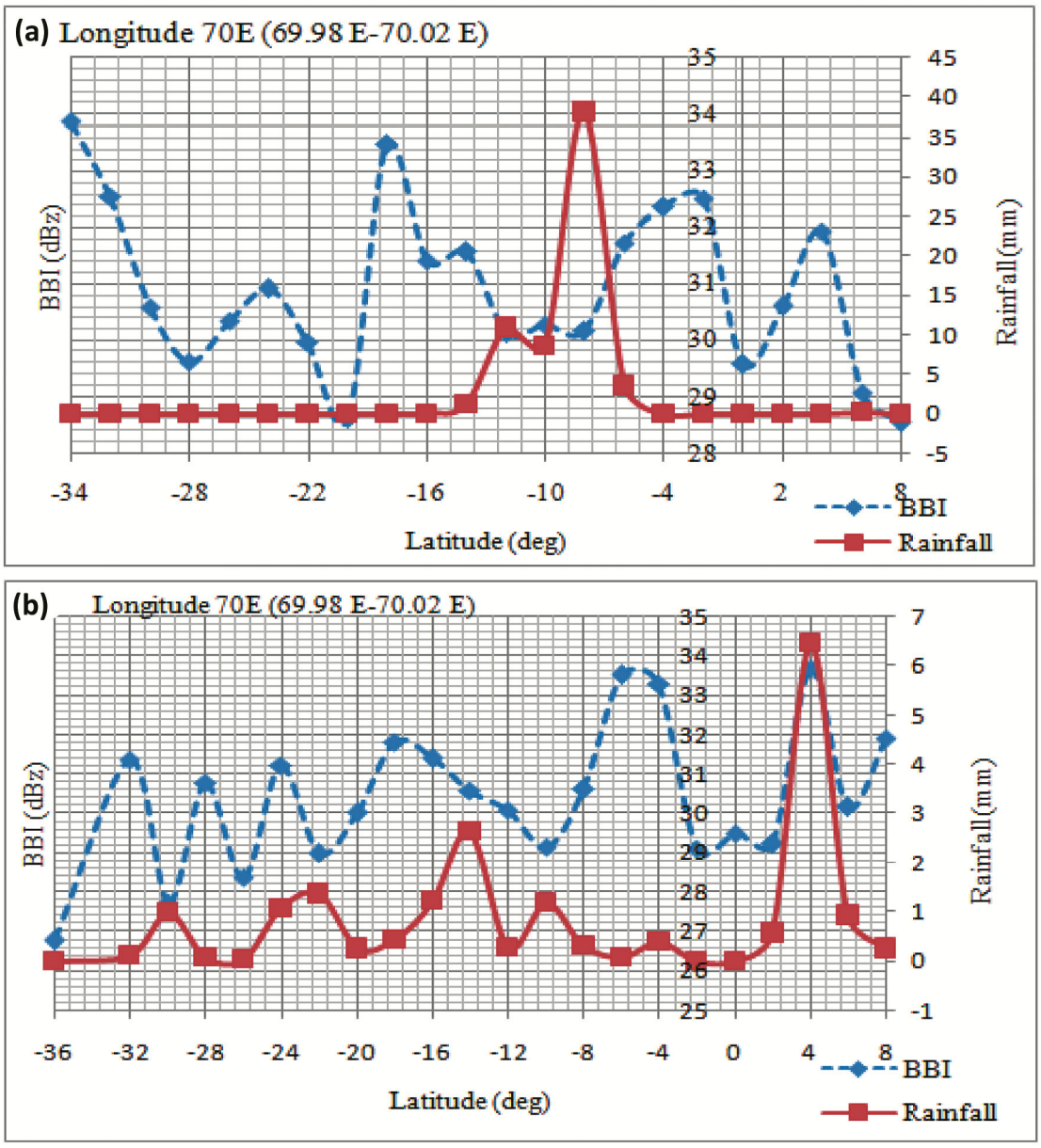

Fig. 5 — Variation of BBI and rainfall with latitude on (a) 1 March 2007, and (b) 15 January 2008

Conclusion

The occurrence of daily BBI_{mx} and BBI_{mn} shows seasonal dependence. These mostly occur over the North Pacific and the South Pacific. Sometimes, it occurs over the North Atlantic also. This indicates that the occurrence of BBI is higher over the North and the South Pacific Oceans than over the continents or other oceanic locations. This, in turn, indicates the formation of drops of larger diameter over the Pacific Ocean in comparison to other oceanic or continental masses. Thus, the North and the South Pacific Ocean appear to play a significant role in causing the radar bright band, and weather formation.

Among the continental mass, the BBI_{mx} mostly occurs over South America, followed by the USA and Africa. The BBI_{mn} mostly occurs in the USA, followed by China and South Africa.

The BBI is higher in the winter hemisphere, where cold and dry weather prevails. The BBI_{mn} belt shows distinct seasonal migration from the southern to the northern hemisphere, and vice versa- an oscillatory motion in a direction opposite to that of the ITCZ, and

that of the Sun. The seasonal oscillation of the BBI_{mx} also resembles the BBI_{mn}. However, it is not as prominent as of BBI_{mn}.

In the NH, the longitudinally averaged BBI_{mx} mostly lies at lower latitudes and at higher latitudes in the SH. Conversely, the longitudinally averaged BBI_{mn} mostly occurs at high latitudes in both hemispheres, indicating the formation of smaller drop sizes in comparison to that of low latitudes.

A higher occurrence of BBI_{mx} or BBI_{mn} over a location does not necessarily mean a greater chance of high rainfall intensity over the location. However, the longitudinally averaged values of BBI and rainfall reveal that the rainfall maxima (minima) and the BBI_{mx} (BBI_{mn}) mostly occur in the same hemisphere. The rainfall is higher in the summer hemisphere. Also, when the rainfall maxima occur in one hemisphere, the minima exist in the other. The BBI minima and maxima also do not occur in the same hemisphere.

Supplementary Data

Supplementary data associated with this article is available in the electronic form at https://or.niscpr.res.in/index.php/IJMS/article/view/2333/621

Acknowledgments

The authors are grateful to Sona College of Technology for supporting the work. The authors sincerely acknowledge the Indian Space Research Organization, and the Government of India, for sponsoring the project under the RESPOND Scheme.

Conflict of Interest

There is no conflict of interest.

Ethical statement

The manuscript has not been submitted elsewhere nor published anywhere. The proposed work is original. The authors have not misinterpreted the results. The presented results do not pose a threat to public health or national security.

Author Contributions

RSJ: Result analysis, manuscript writing, and formatting; SFR: Calculations and plotting of graphs; KTL: Plotting of graphs, preparation of figures, proofreading, and formatting; RM: TRMM data downloading and development of algorithm for data conversion to ASCII; and RD: literature survey, reference formatting, checking of results, table framing and improvement of quality of the figures.

References

1 Battan L J, *Radar Observation of the Atmosphere*, (The University of Chicago Press, Chicago), 1973, pp. 324.

2 Smyth T J & Illingworth A J, Radar estimates of rainfall rates at the ground in bright band and non-bright band events, *Q J R Meteorol Soc*, 124 (1998) 2417-2434.

3 Berenguer M & Zawadzki I, A study of the error covariance matrix of radar rainfall estimates in stratiform rain, *Weather Forecast*, 23 (2008) 1085-1101.

4 Joss J & Waldvogel A, *Radar in Meteorology*, (American Meteorological Society, Boston), 1990, pp. 577.

5 Harrison D L, Driscoll S J & Kitchen M, Improving precipitation estimates from weather radar using quality control and correction techniques, *Meteorol Appl*, 6 (2000) 135-144.

6 White A B, Neiman P J, Martin F, Kingsmill D E & Persson P O G, Coastal orographic rainfall processes observed by radar during the California land-falling jets experiment, *J Hydrometeor*, 4 (2003) 264-282.

7 Lin D, Pickering B & Neely III R R, Relating the radar bright band and its strength to surface rainfall rate using an automated approach, *J Hydrometeor*, 21 (2020) 335-353.

8 Okamoto K, Sasaki H, Deguchi E & Thurai M, Bright band statistics observed by the TRMM precipitation radar, paper presented at the *2nd TRMM International Science Conference*, Nara, Japan, 2004.

9 Ahrens C D, *Essentials of Meteorology*, (Brooks/Cole, Belmont, U.S.A.), 2011, pp. 504.

10 Aguado E & Burt J E, *Understanding Weather and Climate*, (Pearson Prentice Hall, New Jersey), 2010, pp. 586.

11 Girolamo P D, Summa D, Bhawar R, Lorio T D, Vaughan G, *et al.*, Lidar and radar measurements of the melting layer in the frame of the convective and orographically-induced precipitation study, paper presented at the *8th International Symposium on Tropospheric Profiling*, Delft, The Netherlands, 2009.

12 Tokay A & Short D A, Evidence from tropical raindrop spectra of the origin of rain from stratiform versus convective clouds, *J Appl Meteorol*, 35 (1996) 355-371.

13 Shin D B, North G R & Bowman K P, A summary of reflectivity profiles from the first year of TRMM radar data, *J Climate*, 13 (2000) 4072-4086.

14 Sen Jaiswal R, Sonia R F, Rasheed M, Neela V S, Leena Z, *et al.*, Study of radar bright band and freezing level height in 36N-36S region, *Ind J Geo-Marine Sci*, 47 (2018) 1240-1266.

15 Fabry F & Zawadzki I, Long-term radar observations of the melting layer of precipitation and their interpretation, *J Atmos Sci*, 52 (2001) 838-851.

16 Houze R A Jr, Stratiform precipitation in regions of convection: meteorological paradox, *Bull Amer Meteor Soc*, 78 (1997) 2179-2196.

17 Houze R A Jr, Convective and stratiform precipitation in the tropics, In: *Tropical Rainfall Measurements*, edited by J S Theon & N Fugono, (A. Deepak Publishing, Seattle, Washington, USA), 1988, pp. 27-35.

18 Steiner M, Houze R A Jr & Yuter S E, Climatological characterization of three dimensional storm structure from operational radar and rain gauge data, *J App Meteor*, 34 (1995) 1978-2007.

19 Bringi V N & Chandrasekar V, *Polarimetric Doppler Weather Radar: Principles and Applications*, (Cambridge University Press, UK), 2001, pp. 378.

20 Sen Jaiswal R, Sonia R F, Neela V S, Rasheed M & Zaveri L, Study of radar bright band over a tropical station, paper presented at the *Ninth Conference on Coastal Atmospheric and Oceanic Prediction and Processes*, Maryland, U.S.A., 2010.

21 NASA, http://mirador.gsfc.nasa.gov/cgi-bin/mirador/presentNavigation.pl?tree=project & project =TRMM, 1998. Last updated in 2021.

22 Hassiotis A D, Skaropoulos N C & Russchenberg H W J, Quantitative analysis of spectral differential reflectivity in the radar bright band, paper presented at the *Second European Conference on Radar Meteorology*, Delft, Berlin, 2002.

23 Kollias P & Albrecht B, Why the melting layer radar reflectivity is not bright at 94 GHz, *Geophys Res Lett*, 32 (2005) 1-5.

24 Williams C R, Ecklund W L & Gage K S, Classification of precipitating clouds in the tropics using 915 MHz wind profilers, *J Atmos Oceanic Technol*, 12 (1995) 996–1012.

25 Sharma S, Konwar M, Sarma D K, Kalapureddy M C R & Jain A R, Characteristics of rain integral parameters during tropical convective, transition and stratiform rain at Gadanki and its application in rain retrieval, *J Appl Meteorol Clim*, 48 (2009) 1245–1266.

26 Mahen K, Maheskumar R S, Das S K & Morwal S B, Nature of light rain during presence and absence of bright band, *J Earth Syst Sci*, 121 (2012) 947–961.

27 Thurai M, Bringi V, Patrick N G, Walter A P & Matthew T W, Measurements and modeling of the full raindrop size distribution, *Atmosphere*, 10 (2019) 1-16.

28 Zrnic D S, Rain characteristics revealed with the polarimetric radar, paper presented at the *International Symposium on rainfall rate and radio wave propagation*, Tamil Nadu, India, 2007.

29 Kunhikrishnan P K, Sivaraman M R, Kiran Kumar N V P & Denny A, Rain drop size distribution over a tropical Indian station using disdrometer, paper presented at the *International Symposium on rainfall rate and radio wave propagation*, Tamil Nadu, India, 2007.

30 Maitra A, Rain attenuation modeling from measurements of rain drop size distribution in the Indian region, *IEEE Antennas Wirel Propag Lett*, 3 (2004) 180-181.

31 Huggel A, Schmid W & Waldvogel A, Rain drop size distributions and the radar bright band, *J Appl Meteor*, 35 (1996) 1688-1701.

32 Waldvogel A, The N_0 jump of raindrop spectra, *J Atmos Sci*, 31 (1974) 1067-1078.

33 Sarma A C, Deshamukhya A, Rao T N & Sharma S, A study of raindrop size distribution during stratiform rain and development of its parameterization scheme in the framework of multi-parameter observations, *Meteor Appl*, 23 (2016) 254-268.

34 Rossa A, Haase G, Keil C, Alberoni P, Ballard S, *et al.*, Propagation of uncertainty from observing systems into NWP: COST731 Working Group 1, *Atmos Sci Lett*, 11 (2) (2010) 145-152.

35 Awaka J, Iguchi T & Okamoto K, TRMM PR standard algorithm 2A23 and its performance on bright band detection, *J Meteor Soc*, 87A (2009) 31-52.

36 GPM, https://gpm.nasa.gov/missions/GPM, 2022. Last updated in 2019.

37 Stormfax, http://www.stormfax.com/elnino.htm, 2020. Last updated in 2021.

38 Toma E V & Webster P J, Oscillations of the intertropical convergence zone and the genesis of easterly waves Part 1: diagnostics and theory, *Clim Dyn*, 34 (2009) 587-604.